MOLEKUL
eISSN: 2503-0310

Articles
https://doi.org/10.20884/1.jm.2023.18.3.8316

Characteristics of Natural and Acid-Activated Clay from Hatu Village, Mollucas Province: FTIR, XRD, SEM-EDX, XRF, TEM, and BET Analysis

Serly Jolanda Sekewael*, Mirella Fonda Maahury

Department of Chemistry, Faculty of Mathematics and Natural Sciences, Pattimura University, Ambon, Indonesia

*Corresponding author email: sekewaelsj@gmail.com

Received March 24, 2023; **Accepted** August 14, 2023; **Available online** November 20, 2023

ABSTRACT. Research on the chemical and physical characteristics of natural and acid-activated clay from Hatu Village used FTIR, XRD, XRF, SEM-EDX, TEM, and BET surface area analyzer instruments. The natural clay was activated with 0.25 M sulfuric acid for 3 hours using the reflux method, then calcined with 700 Watt microwave radiation for 10 minutes. Overall, FTIR data show tetrahedral and octahedral functional groups that create clay minerals. There was a decrease in absorption peak intensity at 1635; 686; and 470 cm^{-1} due to acid's influence, which dissolves cations in the octahedral and interlayer clay. The XRD analysis shows the Hatu natural clay contains Montmorillonite, alumina, kaolinite, quartz, and illite minerals. Broadening and decreasing the intensity of diffraction peaks of Montmorillonite due to treatment by acid and calcination. SEM images of natural clay before and after activation-calcination show the morphology of porous and layered material, while the mapping of the surface of natural clay shows irregular and rough material topography. The EDX spectra showed four elements with the most extensive composition: O, Si, Al, and Fe. XRF data confirmed three components that have the highest mass percent, namely SiO_2, Al_2O_3, and Fe_2O_3. Dealumination of alumina content of 0.95% occurs due to activation by sulfuric acid along with calcination. TEM images clearly show the multilayered silicate materials. The results of the adsorption-desorption analysis of nitrogen on acid-activated natural clay showed an increase in the specific surface area and total pore volume due to the activation. The characteristics of natural clay from Hatu Village are similar to natural clay from other areas in Indonesia as previously reported by researchers. Activation by sulfuric acid increases the chemical properties of the clay.

Keywords: Acid-activated clay, characteristics, Hatu Village, natural clay

INTRODUCTION

Clay is a layered material, consisting mainly of tetrahedral silica and alumina octahedral sheets that form a single layer, which can be divided into four major groups. These include the kaolinite group, the Montmorillonite/smectite group, the illite group, and the chlorite group with a common characteristic: natural structure fine-grained with sheetlike geometry (Bergaya & Lagaly, 2013). The arrangement of the layers creates a space in which water molecules and ions are filled. Hydrous silicates sheet-structured are generally referred to as phyllosilicates. Diameter particles of natural clay are smaller than 0.004 mm; these can be ranged from 0.002 to 0.001 mm in diameter for quartz, mica, feldspar, iron, and aluminum oxides. Colloidal clay particles are found in finer-layered silicates with a diameter of <0.001 mm (Bergaya & Lagaly, 2013).

Clay minerals are one of the natural materials found in various regions in Indonesia. In Mollucas Province, clay soil had been found in Latuhalat, Hatu, Ouw, and Lonthoir Village. In recent years, research on natural clay from Moluccas Province began to develop (Ikhsan *et al*., 2022). Natural clay from Ouw and Latuhalat Village was dominated by Montmorillonite clay that quickly absorbs water (Bijang *et al*., 2010; Latupeirissa *et al*., 2014). Clay soils play a natural "scavenger" role in removing and collecting contaminants, including heavy metals, in water passing through the soil by ion exchange and adsorption (Bhattacharyya & Gupta, 2007; Zhu *et al*., 2016; Zhang *et al*., 2020; Kinoti *et al*., 2022). Natural clay, especially bentonite can also be used as an absorbent for dyes (Sadiana *et al*., 2018; Said *et al*., 2020) and for ammonium removal (Alshameri *et al*., 2013; Angar *et al*.,2017; Alshameri *et al*., 2017).

Although natural clays are very useful for adsorption, their adsorption capacity is limited. This weakness can be overcome through the activation process using acid (Komadel, 2016). Acid activation of clay minerals probably is one of the most effective methods that has been used to produce active materials for adsorption and catalysis purposes. Clay that has been activated by acid will maintain its thermal stability through a calcination process which

also aims to increase the surface area and enlarge the pore volume of the clay.

The aim of this research is to study the characteristics of natural and acid-activated clay from Hatu Village. Sulfuric acid activates the natural clay followed by calcination to improve the chemical properties of the clay. Sulfuric acid will exchange H^+ cations with cations in natural clay layers during the process, and the result is an increase in the specific surface area of the clay (Bhattacharyya & Gupta, 2007). Sulfuric acid also has a higher H^+ equivalence number than inorganic acids such as HCl, making it more effective in the cation exchange process.

Microwave radiation in this study was used to replace the conventional calcination process. Microwave radiation assists the calcination reaction in order to reduce time and energy requirements (Sekewael *et al*., 2016). The transfer of energy from microwaves to the material in the calcination process occurs through both resonance and relaxation that occur during the fast heating process (Sekewael *et al*., 2016). Microwave radiation guarantees a short contact time between the clay material and the acidic solution so that charge exchange takes place between hydrated layers accompanied by H^+ cation compensation.

Several instruments are used to study the chemical and physical characteristics of natural and acid-activated clay. The characteristics of the natural clay from Hatu Village are expected to be the same as those from other regions in Indonesia. Activation by sulfuric acid will increase the surface area and pore volume of the clay so that it can be used as an adsorbent or catalyst.

EXPERIMENTAL SECTION

Materials and Methods

Natural clay was obtained from Hatu Village, Mollucas Province, Indonesia. Distilled water, H_2SO_4, and $BaCl_2{\cdot}2H_2O$ were employed in this study. Instruments used in this characterization were FTIR type Prestige 21 Shimadzu, X-ray diffractometer (XRD) type XRD Rigaku Miniflex 600, XRF type NEX QC+ Rigaku, Scanning Electron Microscope (SEM) type FEI Inspect S50, Transmission Electron Microscope (TEM) type JEOL 1400 series, and surface area analyzer type Quantachrome-NOVA 11000.

Preparation of Natural and Activated Clay

The natural clay had cleaned from impurities such as plant roots and rocks, then washed with distilled water to remove impurities on the clay surface. The natural clay was soaked in distilled water for 24 hours, and through sedimentation and centrifugation processes, the clay fraction <2 μm was separated from natural clay. The clay fraction was then washed with distilled water, air dried, then dried in an oven at 120°C for 48 hours. Furthermore, the clay was crushed and sieved with a 100-mesh sieve. The natural clay sample was encoded as LH. Twenty grams of clay granules (LH) were refluxed with 200 mL H_2SO_4 0.25 M for 3 hours, adopting the Bhattacharyya and Gupta (2007)'s procedure. The activated natural clay was centrifuged and then washed with demineralized water until it was free from SO_4^{2-} ions. Dilute hydrochloric acid and 5% of $BaCl_2$ are dropped into the washing water to test for sulfate ions until there is no white precipitate of $BaSO_4$. The clay is dried in an oven at 110 °C until a constant weight is obtained and then crushed until smooth and sieved using a 100 mesh sieve. The sieved clay was then calcined using a microwave oven at a power level of 750 watts for 10 minutes following Sekewael *et al*. (2016) and encoded as LHAK.

Characterization of Natural and Activated Clay

Samples under 1 mg were used for FTIR analysis. The materials were homogenized with 100 mg of KBr by pressing, crushing, and forming thin, translucent pellets. The FTIR spectrophotometer's instrument cell is then used to analyze this pellet. To ascertain the absorption of functional groups, the spectra of all samples between 400 and 4000 cm^{-1} were examined.

A total of 0.5 g of the powder sample was compacted into a sample holder which was in the form of a glass chip and then placed in an X-ray diffractometer instrument cell which was operated under the following conditions: an accelerating voltage of 40 kV, current of 30 mA, slit width of 0.05, and speed of 0.02 °/sec. Samples were irradiated by CuKα with λ=1.5406Å. The X-ray diffraction pattern of the sample is recorded from 2θ between 3-70 degrees and comes out as diffractogram data which is further analyzed.

The sample was first covered in Au metal, then put in a holder covered in a layer of carbon, and then subjected to SEM-EDAX analysis using a SE (secondary electron) detector. The SE (secondary electron) detector was run under the following conditions: WD 11.7; spots 3.5; an acceleration voltage of 10.0 kV. A morphological picture of the sample is the form that the data taken as a consequence takes.

Samples for TEM investigation were processed by fixation, incision, and coating procedures. A very high-intensity electron beam that has been accelerated at a voltage of 120 kV bombards the specimen once it has been set up on the TEM grid. The "soft" portions of the specimen allow the electron beam to pass through, but the hard portions (such as particles) of the specimen block the electron beam. The electron beam that exits from the sample's soft area is captured by the detector behind the sample. In turn, the detector provides a picture of the sample under analysis by capturing an image whose shape is identical to the shape of the hard section of the sample (particle shape).

An N_2 gas sorption analyzer was used to examine the samples' porosity. Samples were degassed for three hours at 300 °C in a reduced atmosphere before measurement. Additionally, liquid nitrogen was used to chill each sample, resulting in a thin film of nitrogen

molecules covering each surface. It is possible to calculate the precise surface area, typical pore volume, typical pore radius, and typical pore size distribution.

RESULTS AND DISCUSSION

Natural clay was obtained from Hatu village. The sampling location is located at 03° 42.095' latitude and 128° 04.431' east longitude and an altitude of ± 7 m above sea level. The location is approximately 200 meters from the Wai Sikula River basin. It is similar to watershed locations in general, but there is still a lot of forest tree vegetation surrounding the loam soil area. The local community generally takes clay soil as the raw material for making red bricks. The clay color is grayish red, breaks easily in dry conditions, and has a very sticky texture when held in wet conditions. The appearance of natural clay from Hatu is similar to natural clay from Bayat as reported by Winarno *et al*. (2017). The sticky nature of clay indicates the presence of Montmorillonite minerals. XRD data has provided proof of it. Physically, the color of acid-activated-calcined clay is brighter than natural clay. It is an early indication that sulfuric acid has partially reduced the clay's color.

FTIR Analysis of Natural and Acid-Activated Clays

Figure 1 shows important peaks for natural and acid-activated clay identification. All absorption peaks shown in **Figure 1** are similar to those reported by Bhattacharyya and Gupta, (2007); Sekewael *et al*. (2016); and Pranoto *et al*. (2018).

The absorption at 3618 cm^{-1} shows the stretching vibration peak of the octahedral –OH (Al-OH) structure. According to Acevedo *et al*. (2017), the presence of Montmorillonite in natural clay minerals is indicated by absorption at 3620 cm^{-1} which is a typical Montmorillonite dioctahedral absorption. Meanwhile, the wide peak with moderate intensity at 3448 cm^{-1} is a stretching vibration of the water-OH molecule. An absorption peak strengthens the vibration band of water molecules at the wave number 1635 cm^{-1}. On acid-activated natural clay, the intensity of the bands at 1635 cm^{-1} decreases, showing the modest degradation of the octahedral layer due to the leaching of octahedral cations (such as Al^{3+} and Mg^{2+}) from the clay structure (Musie & Gonfa, 2022).

The peak intensity becomes slimmer and shifts slightly to the shorter wavelength due to the effect of calcination, in which the hydrated group of the water molecule had reduced. The last three bands mentioned above are an indication that natural clay has water-absorbing properties. The water-absorbing property of clay is that natural clay has a large Montmorillonite content. These results are in line with the XRD analysis report to be described earlier. Widening absorption at 3448 and 3425 cm^{-1} is the stretching vibration of the -OH group from the water molecule, also from the -OH group of silanol and aluminol. Sharp absorption at 2368 cm^{-1} belongs to inner OH hydroxyls of illite minerals which is strengthened by the presence of absorption at 918 cm^{-1}. Acevedo *et al*. (2017) reported an absorption of illite mineral at 2361 cm^{-1} corroborated by the presence of absorption at 914 cm^{-1}.

An Absorption at 1026 cm^{-1} shows the stretching vibration of Si-O, slightly shifting to 1033 cm^{-1} due to an increase of Si/Al ratio induced by dealumination. The bending vibration of Si-O-Si appears at 470 cm^{-1} in the tetrahedral layer. The weak absorption band at 532 cm^{-1}, which also corresponds to the Al-Si-O bending vibration, reinforces the characteristic AlIV tetrahedral bending vibration that appears at 756 cm^{-1}. Acevedo *et al*. (2017) reported

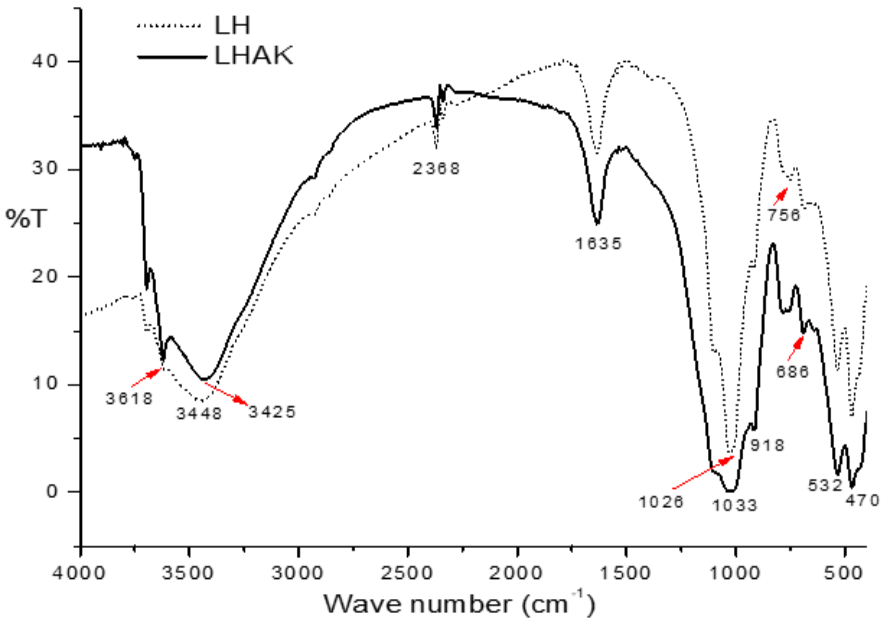

Figure 1. FTIR Spectra of LH and LHAK

an absorption peak at 752-754 cm^{-1} as a perpendicular vibration of Si-O (the characteristic absorption band of kaolinite). Natural clay has a weak absorption at wave number 686 cm^{-1}. This absorption was reported by Acevedo *et al*. (2017) as Si-O-Al (octahedral Al) bending vibrations (the characteristic absorption band of quartz). This fact is confirmed by Tyagi *et al*. (2006), the functional group associated with the quartz component is absorbed at 692 cm^{-1}.

Overall, the infrared spectroscopy data indicate the presence of functional groups of tetrahedral and octahedral sheets that compose natural and acid-activated clay minerals. The two samples have similar absorption patterns, followed by a decrease in intensity and a shift in several absorption bands.

XRD Analysis of Natural and Acid-Activated Clays

The identification of the LH and LHAK samples using the XRD instrument can be seen in Figure 2. The diffractogram of the two samples shows an amorphous natural clay material. In general, the series of diffraction patterns in **Figure 2** shows a stable retention pattern of amorphous material even when treated with sulfuric acid (LHAK). The existence of prominent diffraction peaks that still appear in both samples was proven.

LH has the main diffraction peaks at 2θ respectively, namely: 6.336; 12.69; 21.10; 26.920; 28.235; and 35.21°, respectively a typical reflection of the Montmorillonite (M), allophane (A), kaolinite (K), quartz (Q), and illite (I) phases. The characteristic peaks of natural clay are similar to Bekonang clay as reported by Pranoto *et al*. (2018), and also to Central Kalimantan clay as reported by Sadiana *et al*. (2018). The peak at 2θ = 6.6336 with a base distance of 13.94 Å shows the characteristic peak of Montmorillonite LH, the peak shifts slightly to the left to 2θ = 6.06 and an increase in the base distance to 14.58 Å for LHAK. It can be explained that the activation process of natural clay with acid followed by calcination using microwaves contributes to an increase in the base distance from the clay and a decrease in the intensity of the diffraction peaks (**Figure 2**).

The estimated crystal size values from the Scherrer equation for LH and LHAK are 46.71 and 41.22 nm, respectively. The small size of LHAK crystals is associated with the widening of the reflection peak and the smaller the Montmorillonite plane's diffraction intensity (**Figure 2**). The small crystal size also contributed to the increase in the specific surface area of LHAK (**Table 2**). The results of the XRD analysis agreed with those of the FTIR analysis. Several characteristic absorption peaks of natural clay minerals, such as Montmorillonite, kaolinite, quartz, and illite appear in the XRD diffractogram and are supported by the FTIR spectrum.

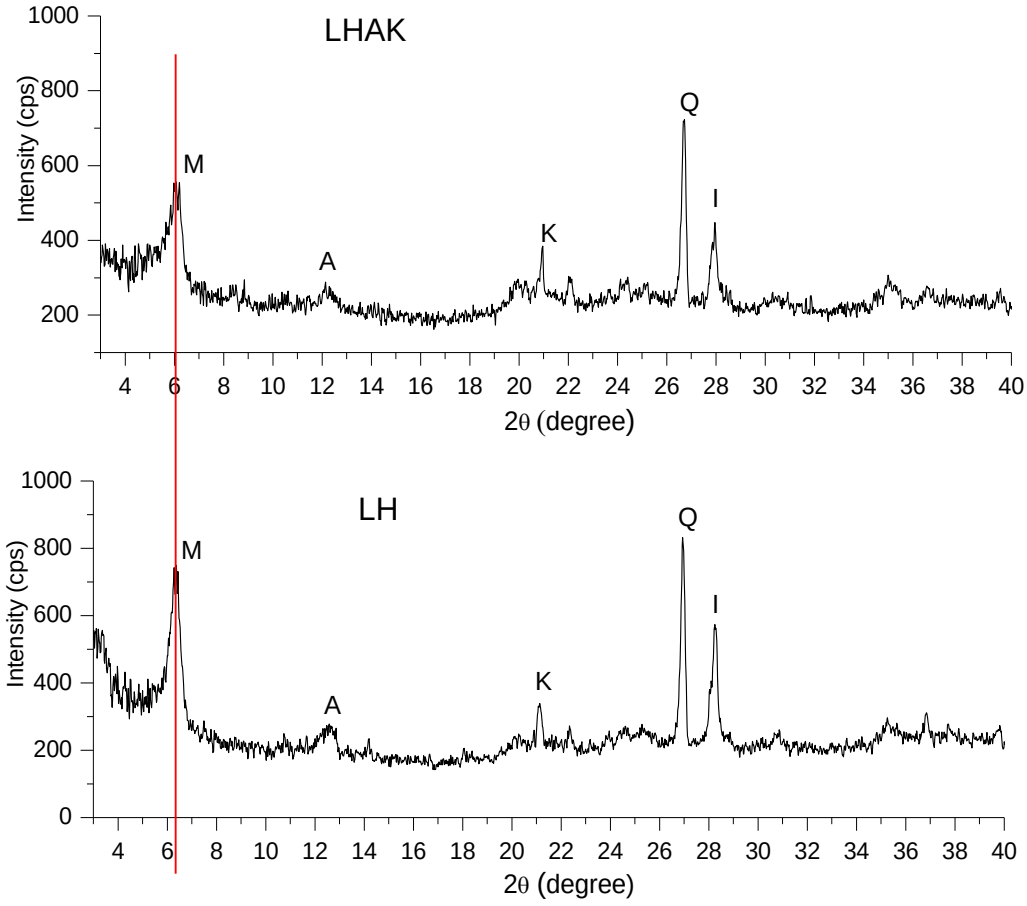

Figure 2. Diffractogram of LH and LHAK

SEM-EDX Analysis of Natural and Acid-Activated Clays

SEM images and EDX spectra of LH and LHAK samples with 5000 magnification are presented in **Figure 3**. SEM images show the analyzed samples' topography and surface morphology, while EDAX shows the constituent elements. Both samples showed typical topography and morphology of porous, layered, irregular, and coarse material. Sekewael *et al*. (2017) have reported this topographical model, especially typical materials containing Montmorillonite. Physically, it can be observed that the surface topography of LHAK shows more pore structures than LH, probably because the activity of washing with acid causes the appearance of new pores in the clay.

The EDX spectra of LH and LHAK (**Figure 3** right) along with elemental analysis (**Table 1**) show the chemical composition of the elements. The four main components are O, Si, Al, and Fe. During the acid treatment, protons penetrate into the mineral layer and attack the structural OH groups resulting in dehydroxylation which is associated with the successive removal of the central atom from the octahedral as well as with the removal of Al from the tetrahedral sheet (Komadel, 2016). The number of Fe and Al elements decreased due to natural clay activation by sulfuric acid (**Table 1**), there was a dealumination of 0.95%.

Table 1. Elemental analysis

Sample	Elements (%)						
	O	Mg	Al	Si	K	Ca	Fe
LH	52.07	2.37	12.39	17.65	0.35	1.00	7.27
LHAK	54.02	1.78	10.87	18.68	0.73	0.29	5.94

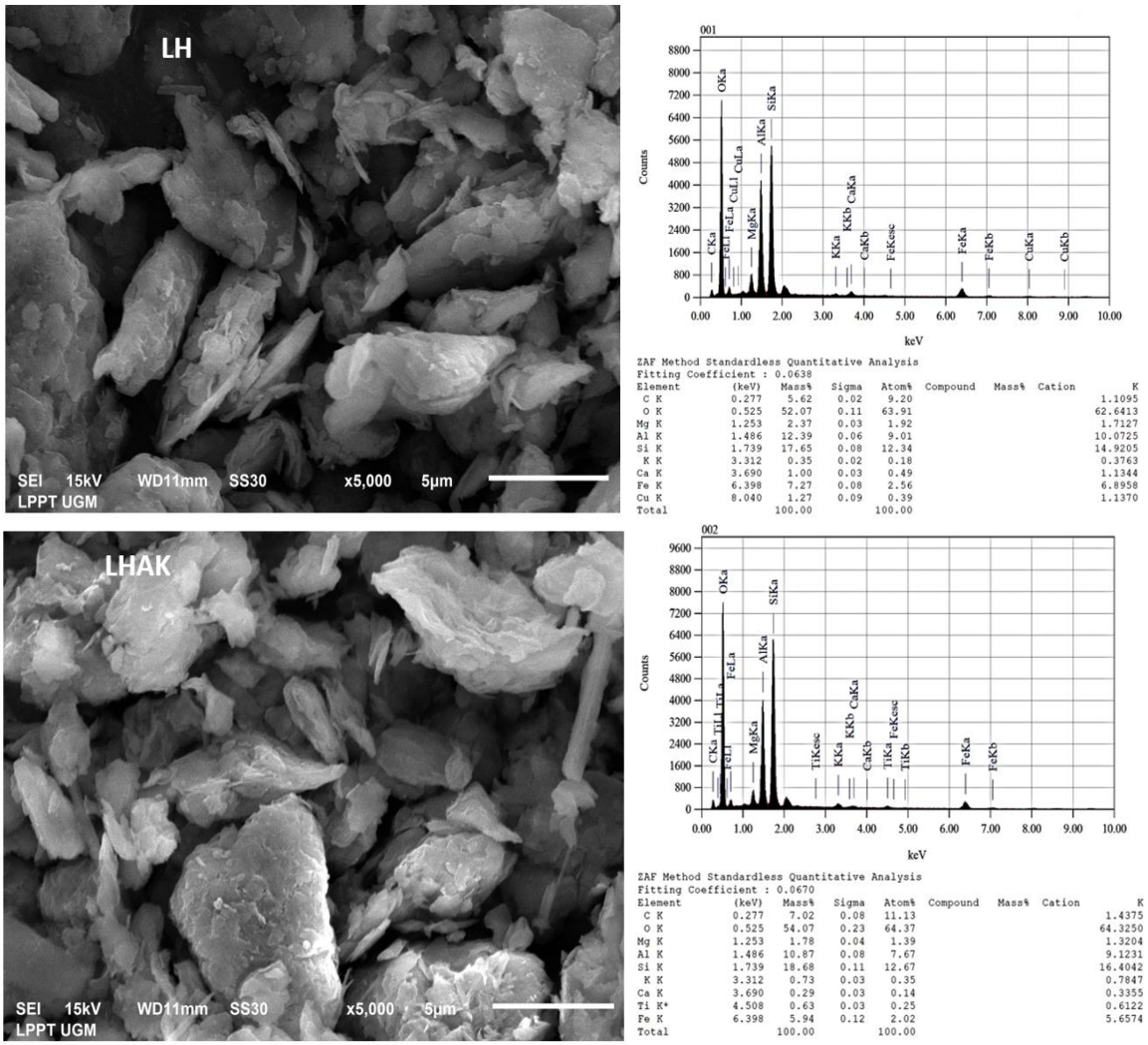

Figure 3. SEM images (left) and EDX spectra (right) of LH and LHAK

XRF Analysis of Natural Clay

XRF analysis results showed the chemical compositions of Hatu natural clay (**Table 2**). **Table 2** shows that alumina and silica oxide are present in large quantities in contrast to other minerals which are only present in small amounts. This confirms the chemical analysis of clay as reported by Yanti and Muhktar (2015) and Winarno *et al*. (2017). The results of the XRF analysis are consistent with the EDX data of Hatu natural clay samples (LH) which show the four highest elemental contents, namely O, Si, Al, and Fe.

TEM Analysis of Natural and Acid-Activated Clays

The morphological characterization of natural clay and natural activated clay with 700 Watt microwave radiation can be seen in **Figure 4**. The arrangement between layers appears but looks irregular due to the delamination structure (shown by yellow arrows). The same results obtained by Yuan *et al*. (2008) stated that the irregularity between clay layers resulted from the delamination structure due to the contribution of mesoporous volume to the clay. The BET data support mesoporous structure (**Figure 6**).

The TEM image of LHAK shows multilayered silica undergoing exfoliation (shown by red arrow) or loss of the layer arrangement of individual clay plates into disoriented aggregates (shown by green arrow). Wallis *et al*. (2007) reported several things after acid activation of Montmorillonite: delaminated structures appear due to dealumination, dislodgement of individual clay plates, and release of cationic constituents into the solution. Komadel (2016) reported that acid activation caused improved exfoliation of the silicate sheets and also increased basal spacing. XRD data reported an increase in basal spacing from 13.94 Å for LH to 14.58 Å for LHAK samples after acid activation and broadening of the Montmorillonite peak (**Figure 2**).

BET Method Analysis of Natural and Acid-Activated Clays

Analysis of nitrogen gas adsorption by both samples is presented in **Table 3**. Natural clay resulting from acid activation (LHAK) has a larger surface area than natural clay before activation and calcination (LH). This result correlates with the small average pore radius of the entire pore surface of 37.21 Å and the small crystal size of 41.22 nm. The reaction of clay minerals with mineral acid solutions, usually HCl or H_2SO_4, is an acid activation process. Musie and Gonfa (2022) reported that the acid activation process aims to obtain a partly dissolved material with a high specific surface area, porosity, and adsorption capacity.

Table 2. Chemical analysis of hatu natural clay

Chemical composition	Al_2O_3	SiO_2	K_2O	CaO	TiO_2	Fe_2O_3	MnO
Weight (%)	23.51	62.10	0.887	1.952	1.126	10.059	0.223

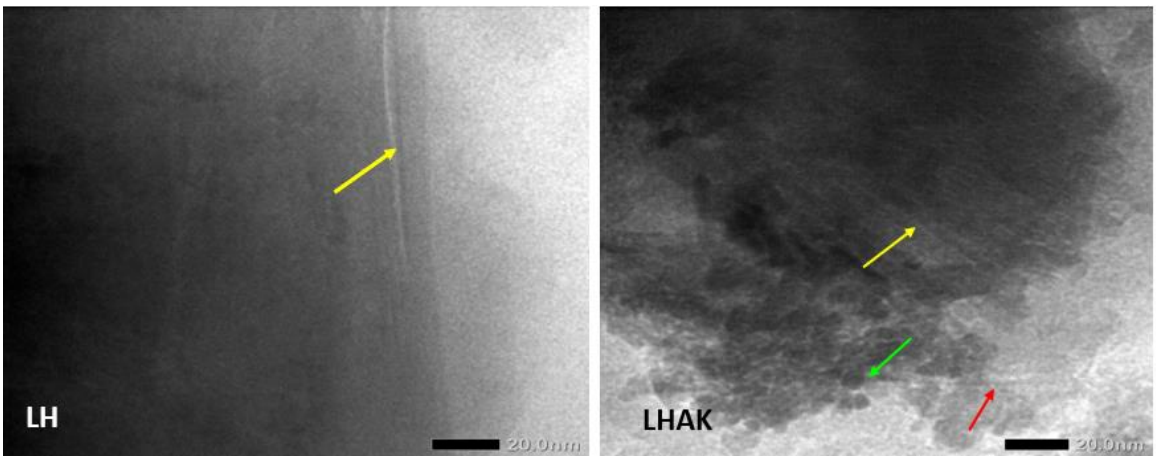

Figure 4. TEM images of LH and LHAK

Table 3. N_2 gas adsorption analysis

Sample	Surface area[a] (m^2g^{-1})	Total pore volume[b] (ccg^{-1})	Average pore radius[b](Å)
LH	12.16	0.035	57.64
LHAK	36.35	0.068	37.21

[a]determined by the multipoint BET method
[b]determined using BJH pore analysis.

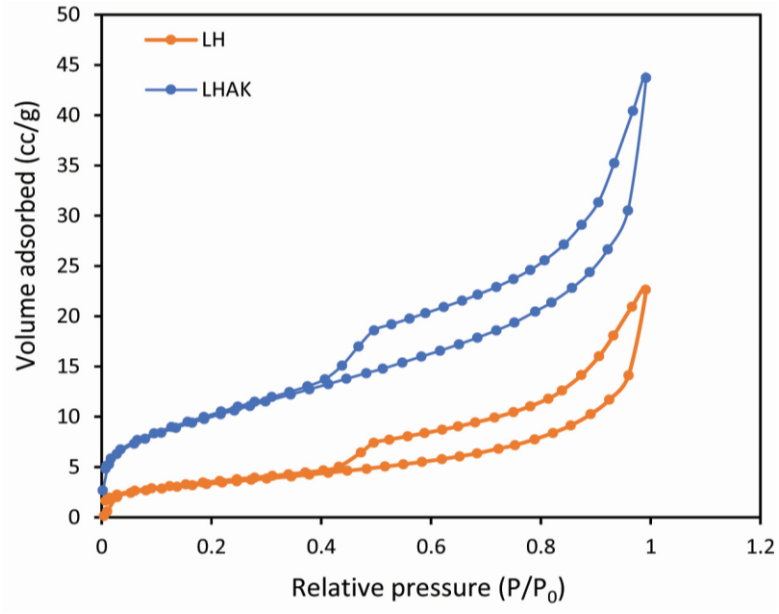

Figure 5. Nitrogen adsorption-desorption isotherm of LH and LHAK

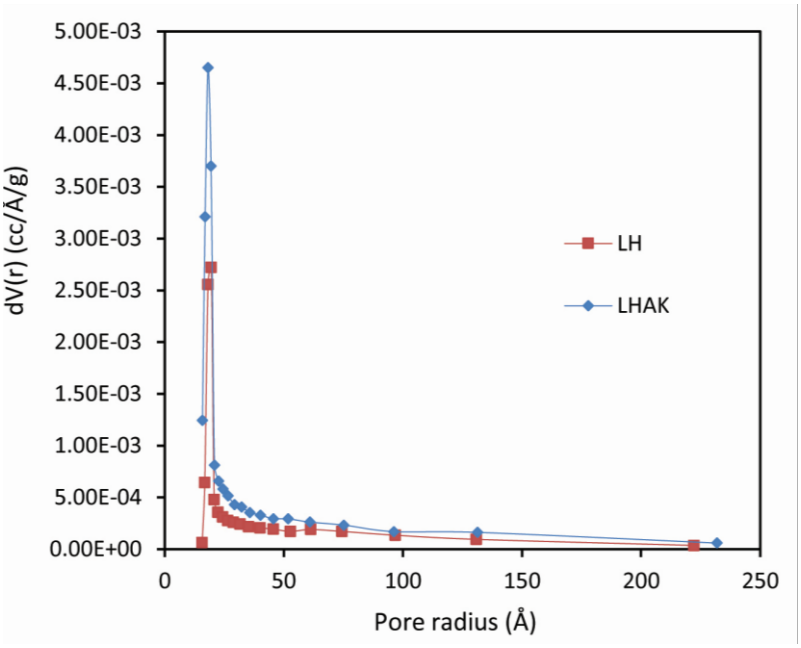

Figure 6. Pore size distribution data of LH and LHAK

The adsorption-desorption isotherm patterns of Hatu natural clay before and after activation are shown in **Figure 5**. Both samples have similar isotherm shapes and patterns. The isotherm pattern follows type IV, which refers to the BDDT classification (Gregg & Sing, 1982). Type IV isotherm is associated with the predominance of mesoporous material. The mesoporous surface of the solid absorbs most of the nitrogen gas. This fact had evidenced by the pore distribution data (**Figure 6**). Adsorption on the mesoporous surface tends to have multilayer formation followed by capillary condensation (type IV adsorption). At relatively low pressures, the adsorption pattern resembles that of macropores, but at relatively high pressures, the amount of adsorbed gas increases sharply with the presence of capillary condensation in the mesoporous. Capillary condensation and evaporation occur at different relative pressures indicating a hysteresis loop. The hysteresis loop follows the H3 type, which refers to the IUPAC classification, indicating slit-shaped pores (Gregg & Sing, 1982). Slit-shaped pores describe the presence of a capillary-shaped gap that is wide enough with a narrow tip.

The adsorption-desorption isotherm in this experimental result clearly shows that nitrogen gas absorption increases continuously. It occurs because the pores of solids are not too narrow to carry more than one molecular layer on the pore walls. On the

other hand, increased mesoporous presence gives an increase in the amount of gas adsorbed. The higher nitrogen gas uptake by LHAK compared to LH was consistent with the large surface area and total pore volume reported in **Table 3**. The larger the surface area, the more nitrogen gas is adsorbed.

Figure 6 shows the pore size distribution pattern of the two samples calculated by the Barrett-Joyner-Halenda (BJH) method. The function f(r), which has a value proportional to the combined volume of all pores whose effective radii are in the minimal range centered on the radius representing the pore size distribution, is the relative abundance of each pore size in the volume representation of the LH and LHAK samples. All samples showed a wide pore size distribution with mesoporous populations dominating the sample solids.

CONCLUSIONS

Characteristics of natural and acid-activated clay from Hatu Village can be described by FTIR, XRD, SEM-EDX, XRF, TEM, and BET analysis, all of which support each other. FTIR data show functional groups from octahedral and tetrahedral sheets that formed clay minerals. The XRD analysis shows the Montmorillonite, alumina, kaolinite, quartz, and illite minerals. SEM images show the morphology of porous and layered material, while the mapping of the surface of natural clay shows irregular and rough material topography. The EDX spectra showed four elements with the most extensive composition: O, Si, Al, and Fe, confirmed by XRF data which showed SiO_2, Al_2O_3, and Fe_2O_3 as three components with the highest mass percent. TEM images clearly show the multilayered silicate materials. The higher nitrogen gas uptake by activated-calcinated natural clay was consistent with the large surface area and total pore volume.

There was an increase in the surface area and pore volume of natural Hatu clay due to activation by sulfuric acid and through the calcination process with microwave radiation assisted. Furthermore, Hatu natural clay and acid-activated clay can be applied as an adsorbent for heavy metals or as an acid catalyst.

ACKNOWLEDGEMENTS

We are pleased to thank Wajumi Takimpo, Idham Olong, and Dewi Sri as laboratory assistants and technicians at the physical chemistry laboratory, Department of Chemistry, Faculty of Mathematics and Natural Sciences, Pattimura University, for their assistance in the sampling process and laboratory assistance.

REFERENCES

Acevedo, N. I. A., Rocha, M. C. G., & Bertolino, L. C. (2017). Mineralogical characterization of natural clays from Brazilian Southeast region for industrial applications. *Cerâmica, 63*, 253–262. http://dx.doi.org/10.1590/0366-69132017633662045

Alshameri, A., Abood, A.R., Yan, C., & Muhammad, A. M. (2013). Characteristics, modification, and environmental application of Yemen's natural bentonite. *Arabian Journal of Geosciences*, *7* (3), 841–853. https://doi.org/10.1007/s12517-013-0855-z.

Alshameri, A., He, H., Zhu, J., Xi, Y., Zhu, R., Ma, L., & Tao, Q. (2017). Adsorption of ammonium by different natural clay minerals: Characterization, kinetics, and adsorption isotherms. *Applied Clay Science*, *159*, 83–93. https://doi.org/10.1016/j.clay.2017.11.007.

Angar, Y., Djelali, N. E., & Kebbouche-Gana, S. (2017). Investigation of ammonium adsorption on Algerian natural bentonite. *Environmental Science and Pollution Research*, *24*, 12, 11078–11089. https://doi.org/10.1007/s11356-016-6500-0.

Bergaya, F., & Lagaly, G. (2013). Chapter 1 - General Introduction: Clays, Clay Minerals, and Clay Science. *Developments in Clay Science*, *5*, 1–19. https://doi.org/10.1016/B978-0-08-098258-8.00001-8.

Bhattacharyya, K. G., & Gupta, S. S. (2007). Adsorptive accumulation of Cd(II), Co(II), Cu(II), Pb(II), and Ni(II) from water on Montmorillonite: Influence of acid activation. *Journal of Colloid and Interface Science, 310*, 411–424. http://dx.doi.org/10.1016/j.jcis.2007.01.080.

Bijang, C., & Sekewael, S. J. (2010). Aktivasi asam lempung Desa Ouw, Saparua, dan aplikasinya sebagai adsorben logam Pb (Activation of clay acid in Ouw Village, Saparua, and its application as a Pb metal adsorbent). *Prosiding,* SNHKI, UNHAS.

Gregg, S. J., & Sing, K. S. W. (1982). *Adsorption, Surface Area, and Porosity*. Academic Press, London.

Ikhsan, N., Sekewael, S. J., & Hasanela, N. (2022). Kinetics and isotherm study of ion phosphate adsorption by Lontor natural clay. *Indonesian Journal of Chemical Research*. *9* (3), 171–178. https://doi.org/10.30598//ijcr.2022.9-ikh.

Kinoti, I.,K., Karanja, E.,M., Nthiga, E.,W., M'thiruaine, C.,M., & Marangu, J. M. (2022). Review Article: Review of clay-based nanocomposites as adsorbents for the removal of heavy metals. *Hindawi Journal of Chemistry*, *2022*, 1–25. https://doi.org/10.1155/2022/7504626.

Komadel, P. (2016). Acid-activated clays: Materials in continuous demand. *Applied Clay Science*. *131*, 84–99. http://dx.doi.org/10.1016/j.clay.2016.05.001.

Latupeirissa, J., & Fransina, E. G. (2014). Karakterisasi lempung asal Desa Latuhalat yang teraktivasi amonium nitrat. *Indonesian*

Journal of Chemical Research, *1*(2), 78–82. https://ojs3.unpatti.ac.id/index.php/ijcr/article/view/75/52.

Musie, W., & Gonfa G., (2022). Adsorption of sodium from saline water with natural and acid activated Ethiopian bentonite. *Results in Engineering*, *14*, 1–10. https://doi.org/10.1016/j.rineng.2022.100440.

Pranoto, P., Purnawan, C, & Utami, T. (2018). Application of bekonang clay and andisol soil composites as copper (II) metal ion adsorbent in metal crafts wastewater. *Rasāyan Journal of Chemistry*, *11*, (1), 23–31. http://dx.doi.org/10.7324/RJC.2018.1111939.

Sadiana, I. M., Karelius, Agnestisia, R., & Fatah, A. H. (2018). Studies on synthesis, characterization, and adsorption of cationic dyes from aqueous solutions using magnetic composite material from natural clay in Central Kalimantan, Indonesia. *Molekul, 13*. (1), 63–71. doi:10.20884/1.jm.2018.13.1.414.

Said, M., Dian, A. R., Mohadi, R., & Lesbani, A. (2020). Cr/Al pillared bentonite and its application on congo red and direct blue removal. *Molekul*, *15*, (3), 140–148. https://doi.org/10.20884/1.jm.2020.15.3.594.

Sekewael, S.,J., Wijaya, K., Triyono, & Budiman, A. (2016). Microwave-assisted preparation and physicochemical properties of mixed oxides silica-zirconia Montmorillonite K10 nanocomposite. *Asian Journal of Chemistry, 28* (10), 2325–2330. http://dx.doi.org/10.14233/ajchem.2016.19982.

Sekewael, S.J., Wijaya, K., Triyono, & Budiman A. (2017). Nanocomposite of modified Montmorillonite K10 with SiO_2-Fe_2O_3 as a catalyst of biodiesel synthesis. *International Journal of ChemTech Research*, *10*, (1), 62–70. https://www.sphinxsai.com/2017/ch_vol10_no1/1/(62-70)V10N1CT.pdf.

Tyagi, B., Chudasama, C.D., Jasra, R.,V. (2016). Determination of structural modification in acid activated montmorillonite clay by FT-IR spectroscopy. *Spectrochimica Acta Part A*, *64*, 273–278.

Wallis, J. P., Gates, W. P., Patti, A. F., Scott, J. L., Teoh, E. (2007). Assessing and improving the catalytic activity of K-10 montmorillonite. *Green Chemistry, 9*, 980–986.

Winarno, T., Kurniasih, A., Marin, J., & Kusuma, I. A. (2017). Identifikasi jenis dan karakteristik lempung di Perbukitan Jiwo, Bayat, Klaten dan arahannya sebagai bahan galian industri (Identification of the types and characteristics of clay in the Jiwo Hills, Bayat, Klaten and their direction as industrial minerals). *Teknik*, *38* (2), 65–70. http://ejournal.undip.ac.id/index.php/teknik.

Yanti P.H. & Muhktar A. (2015). Karakterisasi lempung alam Desa Gema teraktivasi fisika (Characterization of natural clay in Gema Village activated by physics). *Chemistry Progress*, *8*, (1), 1–5. https://doi.org/10.35799/cp.8.1.2015.9396.

Yuan, P., Bergaya, F. A., Tao, Q., Fan, M., Liu, Z., Zhu, J., He, H., & Chen, T. (2008). A Combined study by XRD, FTIR, TG, and HRTEM on the structure of delaminated Fe-intercalated/pillared clay. *Journal of Colloid and Interface Science, 324*, 142–149. http://dx.doi.org/10.1016/j.jcis.2008.04.076.

Zhang, T., Wang, W., Zhao, Y., Bai, H, Wen, T, Kang, S., Song, G., Song, S., & Komarneni, S. (2020). Review: Removal of heavy metals and dyes by clay-based adsorbents: From natural clays to 1D and 2D nano-composites. *Chemical Engineering Journal*, *420*, (2), 1–107. https://doi.org/10.1016/j.cej.2020.127574.

Zhu, R., Chen, Q., Zhou, Q., Xi, Y., Zhu, J., & He, H. (2016). Adsorbents based on Montmorillonite for contaminant removal from water: A review. *Applied Clay Science*, *123*, 239–258. https://doi.org/10.1016/j.clay.2015.12.024.